July 21, 2009

Cavitation and Fracture Behavior of Polyacrylamide Hydrogels

Santanu Kundu
Alfred Crosby, *University of Massachusetts - Amherst*

Cavitation and fracture behavior of polyacrylamide hydrogels

Santanu Kundu† and Alfred J. Crosby*

Received 11th May 2009, Accepted 2nd July 2009
First published as an Advance Article on the web 21st July 2009
DOI: 10.1039/b909237d

The mechanical properties of gels present qualitatively contradictory behavior; they are commonly soft but also notoriously brittle. We investigate the elasticity and fracture behavior of swollen polymer networks using a simple experimental method to induce cavitation within a gel and adapt scaling theories to capture the observed transition from reversible to irreversible deformations as a function of polymer volume fraction. It is shown quantitatively that the transition from reversible cavitation to irreversible fracture depends on the polymer volume fraction and an initial defect length scale. The use of cavitation experiments permits characterization of network properties across length scales ranging from μm to mm. We anticipate that these results may significantly enhance the understanding of mechanical properties of soft materials, both synthetic and biological.

Introduction

Understanding the mechanical behavior of gels is critical for an extensive and growing range of applications, from food[1] to engineered tissues.[2] In many respects, gels present qualitatively contradictory behavior; they are commonly soft but also notoriously brittle. Recently, great efforts have focused on developing gels[3] to overcome this contradiction for applications such as cartilage replacement materials,[4] where toughness and high compliance are required. In this paper, we probe the molecular link between the elastic modulus and fracture strength of a swollen gel. We consider this link in the context of a simple observation involving the inflation of a bubble. Bubble formation, or cavitation, has been considered classically for fluids.[5] In contrast, for an extensive elastic network cavitation has been studied less. For elastic gels, the pressurization of a defect (introduced at an arbitrary location) will either cause the network chains to deform rapidly to accommodate an elastic instability, commonly called cavitation, or to rupture in unstable fracture. Interestingly, both deformation mechanisms occur at a critical pressure that scales with the modulus of the elastic network, but in one event the deformation is elastic, and for the other the deformation results in ultimate failure of the material. Both of these reversible and irreversible deformation processes depend on the polymer volume fraction and the length scale of the initial defect.

Scaling theories relating the volume fraction and elastic modulus of a swollen network have evolved over the past few decades.[6–8] Panyukov developed a theory based on the premise that a swollen network constitutes a space-filling system of blobs, as described by de Gennes for polymer solutions.[8,9] Obukhov *et al.* extended this idea to define the modulus of swollen networks for theta and good solvent conditions as a function of the polymer volume fraction (ϕ).[7] For strongly cross-linked networks at theta solvent conditions, the elastic modulus (E) is:

$$E \approx \frac{3kT}{b^3 N}\phi_0^{\frac{2}{3}}\phi^{\frac{1}{3}} \quad (1)$$

where ϕ_0 is the polymer volume fraction at the point of cross-linking, consistent with the result of James and Guth when $\phi_0 = 1$.[6] Here, b is the Kuhn length and N is average degree of polymerization between network junctions. Therefore, as the volume fraction of polymer decreases and swelling increases, the elastic modulus of the swollen material decreases. For good solvent conditions:

$$E \approx \frac{3kT}{b^3 N}\phi_0^{\frac{5}{12}}\phi^{\frac{7}{12}} \quad (2)$$

These scaling relations assume that the distance between network junctions is defined by the density of permanent cross-link points, but for weakly crosslinked networks the density of network junctions contributing to elasticity is defined by the polymer entanglement density, as detailed by Obukhov *et al.*[7] In summary, for $\phi = \phi_0$, all of the these scaling relationships indicate that:

$$E \approx \left(\frac{3kT}{b^3 N}\right)\phi \quad (3)$$

Compared with elasticity, the fracture properties of swollen polymer networks have been studied to a much lesser extent.[10,11] This deficiency is undoubtedly linked to the inherent fragility of swollen polymer networks and the associated difficulty in conducting experimental investigations. According to classical fracture theory, fracture in an elastic solid propagates when the applied energy release rate G, or the change in stored energy per change in fractured area, exceeds a critical value G_c, a material property. For crosslinked polymer networks at $\phi_0 = 1$, Lake and Thomas noted that G_c is not limited by the dissociation energy for the backbone of a polymer chain segment, but must account for the connectivity of the network.[12] In other words, the energy stored in all bonds between network junctions is released when a single bond along the chain segment ruptures. Thus, $G_c \approx NUf$

Polymer Science and Engineering, University of Massachusetts, Amherst, MA, USA. E-mail: santanuk@mail.pse.umass.edu; crosby@mail.pse.umass.edu; Fax: +1 413 545-0082; Tel: +1 413 577-1313
† *Present address*: National Institute of Standards and Technology, Gaithersburg, MD, USA

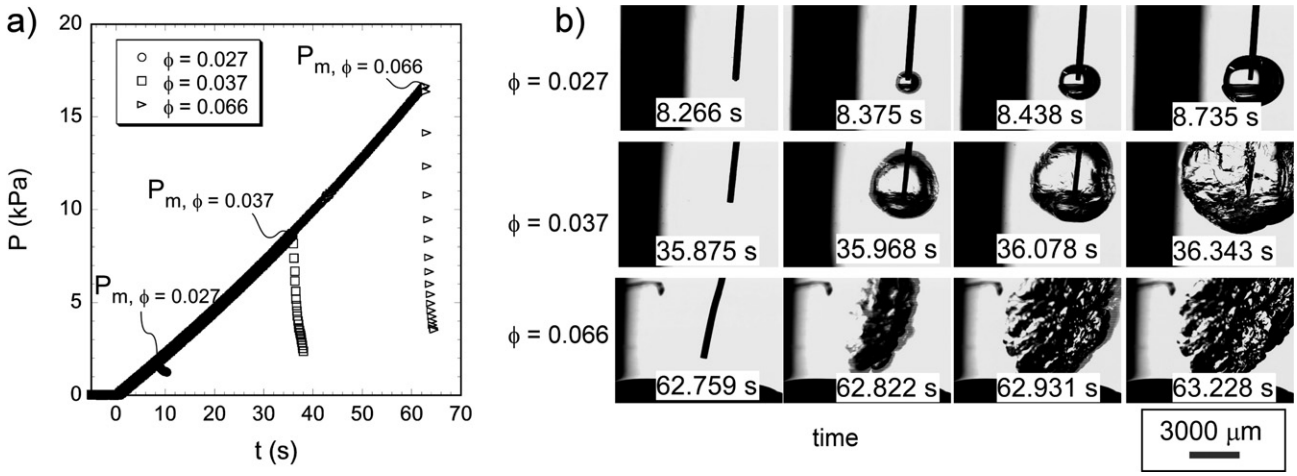

Fig. 1 Transition from cavitation to fracture with the changing polymer concentration. (a) Pressure response for three different gels with volume fraction (ϕ) of 0.027, 0.037, and 0.066. (b) Micrographs of initiation, growth, and propagation of cavitation/fracture at the syringe needle tip. The syringe needle radius is 125 μm.

where U is the dissociation energy for a single bond and f is the areal chain density. Using this framework and building upon the "blob" picture for polymer networks presented by Panyukov[8] and Obukhov *et al.*,[7] we can define $f \approx \nu R$ where the chain density $\nu \approx \phi/Nb^3$ and the chain segment length $R \approx bN^{1/2}$ and $R \approx bN^{1/2}\phi^{-1/8}$ for theta and good solvents, respectively. Substituting these scaling relationships, we obtain $G_c \approx UN^{1/2}\phi/b^2$ for theta solvents and $G_c \approx UN^{1/2}\phi^{7/8}/b^2$ for good solvents. The scaling relationships for elastic modulus and energy release rate provide insight into how network properties change upon swelling, but the performance of gels is dictated by how these properties define the deformation of a network defect, which has a defined length scale.

In this paper, we make use of a simple experiment, cavitation rheology, recently introduced by Zimberlin *et al.*[13] to investigate these scaling relationships and how they define the deformation behavior of a model swollen polymer network, polyacrylamide hydrogels.‡ The experiment involves inserting a syringe needle into a gel at an arbitrary location, ensuring minimum stretching/compression of gels. We pressurize the air within the syringe needle *via* an automated syringe pump and the change of pressure with respect to time is recorded as the syringe volume is compressed. Corresponding changes in the gel at the tip of the syringe needle, *viz.* initiation and growth of cavity/fracture, are imaged using a microscope with a video camera attached. At a critical pressure, the gel at the tip of the syringe needle deforms rapidly. We demonstrate that the nature of this rapid deformation, either reversible cavitation or irreversible fracture, is dictated by the balance of polymer volume fraction and the inner radius of the syringe. These measurements not only provide critical insight into the balance of elastic and fracture properties in swollen gels but also demonstrate the robustness of a simple experimental procedure for quantifying these typically difficult to measure materials properties at small length scales and arbitrary locations.

‡ The polyacrylamide hydrogels were prepared using standard free-radical polymerization with bisacrylamide as the crosslinker. The monomer amount was varied to obtain gels with different polymer volume fraction (ϕ). The monomer to crosslinker ratio was kept constant at 30 for all samples. The experiments were performed under the same swelling conditions as the point of crosslinking ($\phi = \phi_0$). The needle was inserted under closed pressure conditions, thus minimizing gel entering the needle.

Results and discussion

Fig. 1 displays typical pressure responses as a function of time for three different gels with polymer volume fraction (ϕ) of 0.027, 0.037, and 0.066. In all cases, pressure (P) increased linearly with time (t) to a maximum value (P_m) and then dropped instantaneously. As observed in the micrographs, P_m corresponds to the sudden growth of a cavity. Before cavity growth, P is approximately linear with t and independent of material properties[13](Fig. 1). Since experiments were performed in a closed system, the sudden increase in volume associated with the growth of a cavity at the needle's tip resulted in the pressure drop at P_m. As the images in Fig. 1 indicate, the nature of the cavity associated with P_m changes as the polymer volume fraction increases. For $\phi = 0.027$, the cavity is smooth and spherical as opposed to rough and irregular for $\phi = 0.066$ gel, reminiscent of a brittle fracture process. In addition to roughness, the shape of the deformation zone is more planar, similar to a penny-shaped crack. For $\phi = 0.037$, the cavity displayed attributes of both, suggesting a transition in the dominant deformation mechanism as polymer volume fraction increases from 0.027 to 0.066.

Cavitation in elastic polymer networks has been considered from a continuum mechanics perspective.[14,15] At the tip of a syringe, we consider the scheme in Fig. 2(a). Pressurization results in the development of a spherical cap of radius of curvature R and height h at the tip of needle of inner radius, r_s, the initial defect length scale. The work of pressurization (dW) is equal to the sum of the change of elastic energy (dU_E) and surface energy (dU_s), *i.e.*, $dW = dU_E + dU_s$.[15] For the present system, we obtain $PdV = \gamma dA + \sigma dV$, where γ is the surface energy and σ is the material stress surrounding the tip of the needle defined by the appropriate strain energy function for the solid material. For Neo-Hookean materials with Poisson's ratio of 0.5:[14,15]

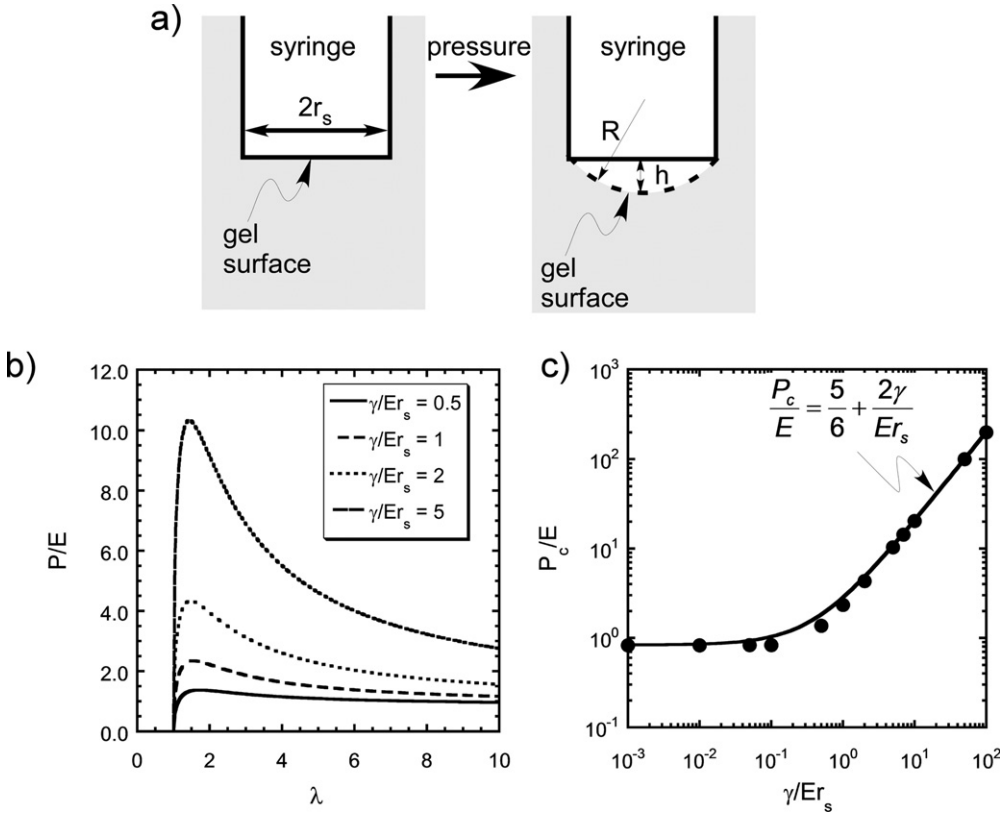

Fig. 2 (a) Schematic represents the cavitation phenomenon observed at the tip of the needle during pressurization. The cavity can be represented as a spherical cap with radius of curvature R and height h. The inner radius of the needle is r_s. (b) P/E, pressure (P) normalized against elastic modulus (E), displays a maximum with the increase of expansion ratio, λ for different values of γ/Er_s. λ is defined as $(A_c/A_{co})^{1/2}$, where A_c is the area of the spherical cap at the tip of the needle and A_{co} is the inner cross-sectional area of syringe. γ/Er_s represents the ratio of surface energy to the elastic energy. (c) Solid data points indicate maximum values of P/E as a function of γ/Er_s. The solid line represents a model fit.

$$P \cong \gamma \frac{dA}{dV} + E\left[\frac{5}{6} - \frac{2}{3}\lambda^{-1} - \frac{1}{6}\lambda^{-4}\right] \quad (4)$$

Here, P is the pressure required to inflate the gel at the tip of the needle to a spherical cap with surface area A_c such that the expansion ratio is defined as $\lambda = (A_c/A_{co})^{1/2}$, and A_{co} is the inner cross-sectional area of syringe (initial area). E is the tensile modulus of the gel. The above equation can be simplified in terms of λ:

$$\frac{P}{E} \cong \left(\frac{4\gamma}{Er_s}\right)\left(\frac{(\lambda^2-1)^{1/2}}{\lambda^2}\right) + \left(\frac{5}{6} - \frac{2}{3\lambda} - \frac{1}{6\lambda^4}\right) \quad (5)$$

As shown in Fig. 2(b), for different values of γ/Er_s, the normalized pressure, P/E goes through a maximum with increasing expansion ratio (λ). This maximum, denoted as P_c/E, is related to the onset of an elastic instability, cavitation. P_c/E increases linearly with γ/Er_s, as shown in Fig. 2(c) where calculated P_c/E values are plotted and fit to:

$$\frac{P_c}{E} = \frac{5}{6} + \frac{2\gamma}{Er_s} \quad (6)$$

This 'cavitation' equation predicts the maximum pressure for defect growth (or cavitation) as a function of initial defect size and materials properties. It is evident that the maximum pressure $P_c/E \rightarrow 5/6$ as elasticity dominates or a larger syringe is used. This relationship has been confirmed experimentally by Gent for a select range of Neo-Hookean elastomers,[14] and more recently by Zimberlin *et al.*[13] for swollen gels. As the initial defect size decreases or the modulus decreases, the surface energy contribution plays a larger role and P_c is defined by a balance of both bulk elasticity and surface energy. We have used needles with different inner radius for a gel with $\phi = 0.027$ and fit the 'cavitation' equation with the experimental results. As shown in Fig. 3, the equation fits well with the experimental results and the corresponding estimated modulus value is 2650 Pa, in close agreement with independent measurements discussed below.

For $\phi > 0.03$ in Fig. 3, the data do not follow a linear increase with $1/r_s$. As opposed to cavitation, fracture in a swollen polymer network will occur when the applied energy release rate equals or exceeds G_c. Assuming that the inner syringe needle radius r_s serves as the length scale governing initial crack growth, the critical pressure for fracture growth is:[15]

$$P_f = \left(\frac{\pi E G_c}{3}\right)^{\frac{1}{2}}\left(\frac{1}{r_s}\right)^{\frac{1}{2}} \quad (7)$$

Shown in Fig. 3, the predicted $P_m \sim r_s^{-1/2}$ holds for gels with $\phi > 0.03$.

The change in scaling for P_m with r_s suggests that the deformation mechanism for low volume fractions is associated with

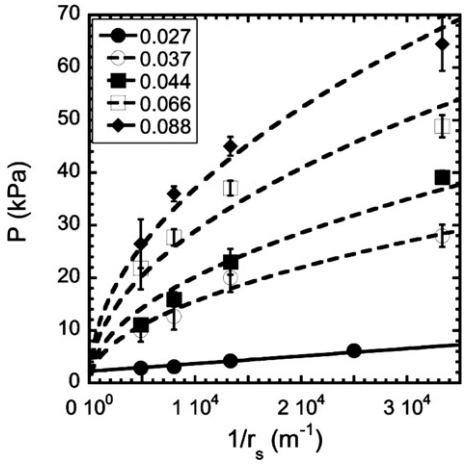

Fig. 3 Maximum pressure (P) as a function of syringe radius for the gels with different volume fraction. For $\phi = 0.027$, P scales linearly with $1/r_s$, whereas for other gels $P \sim r_s^{-1/2}$.

cavitation, a reversible process, while higher volume fractions experience fracture, an irreversible process associated with chain scission, prior to cavitation. This transition from cavitation to fracture is not only dependent upon the volume fraction but also r_s as discussed below.

Reversibility of cavitation phenomenon was verified for a sample with $\phi = 0.027$ by running the syringe pump in multiple pressurization and depressurization cycles (Fig. 4). The cavitation in the second and third cycles occurred at similar pressure compared to the initial cavitation. In contrast, the fracture process was irreversible, suggesting chain scission.

Both the irreversibility and the observed scaling of P_f for gels with $\phi > 0.03$ suggest that P_f measurements from this simple experiment can be used to determine G_c. Rearranging eqn (7):

$$G_c \approx \frac{3P_f^2 r_s}{\pi E} \tag{8}$$

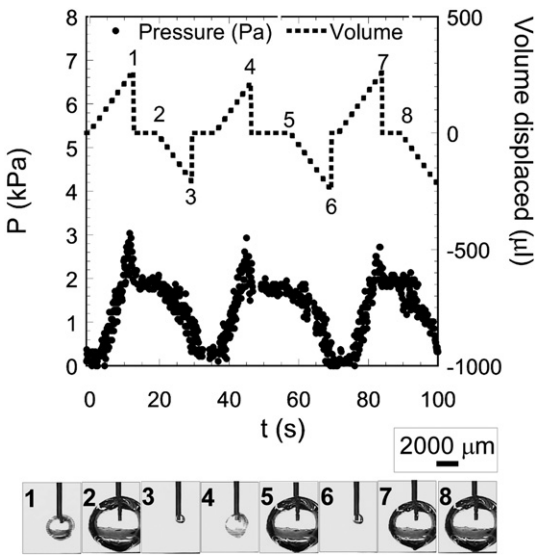

Fig. 4 Reversible cavitation process for $\phi = 0.027$. Pressurization and depressurization was performed multiple times. The cavitation event was observed at similar pressure.

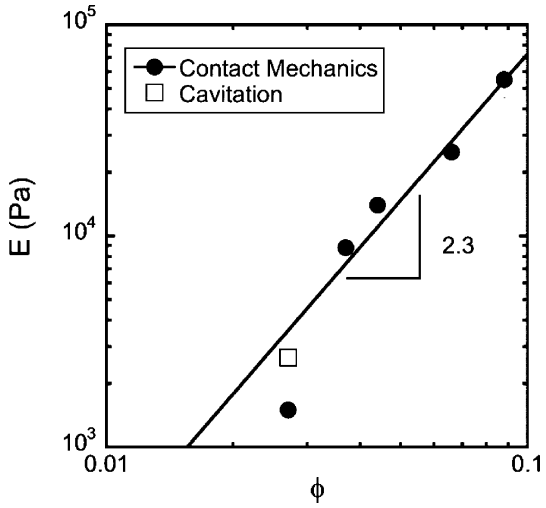

Fig. 5 Elastic modulus as a function of volume fraction. Solid data points are the results from contact mechanics, whereas the open square is the result from cavitation experiments.

Therefore, contact mechanical tests[16] were performed to determine E independently and allow G_c to be quantified. In these tests, the gels were compressed using a cylindrical probe of 2 mm diameter and the corresponding force *vs.* displacement curve was recorded. The modulus of the gel was calculated from the slope of the force *vs.* displacement curve using standard contact mechanics relations.[16] Resulting values of E are shown in Fig. 5. Using these measured values of E, we use the above-stated relationship to determine G_c, as plotted in Fig. 6. These measured values agree well with published values for similar polyacrylamide hydrogels.[11]

From these measurements, it is evident that for swollen gels, the modulus scales strongly with the polymer volume fraction while the fracture toughness, or G_c, scales weakly. This contrast in the volume fraction dependence of critical materials properties provides great insight into the inherent brittleness of many swollen hydrogels. Although the scaling relationships discussed above indicated that both properties should scale with polymer

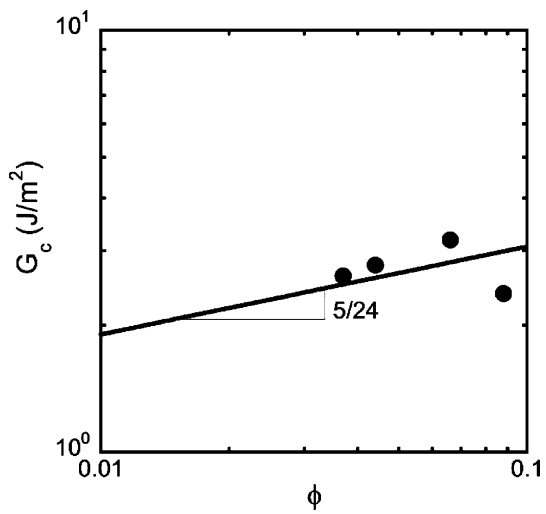

Fig. 6 Estimated values of G_c as a function of volume fraction.

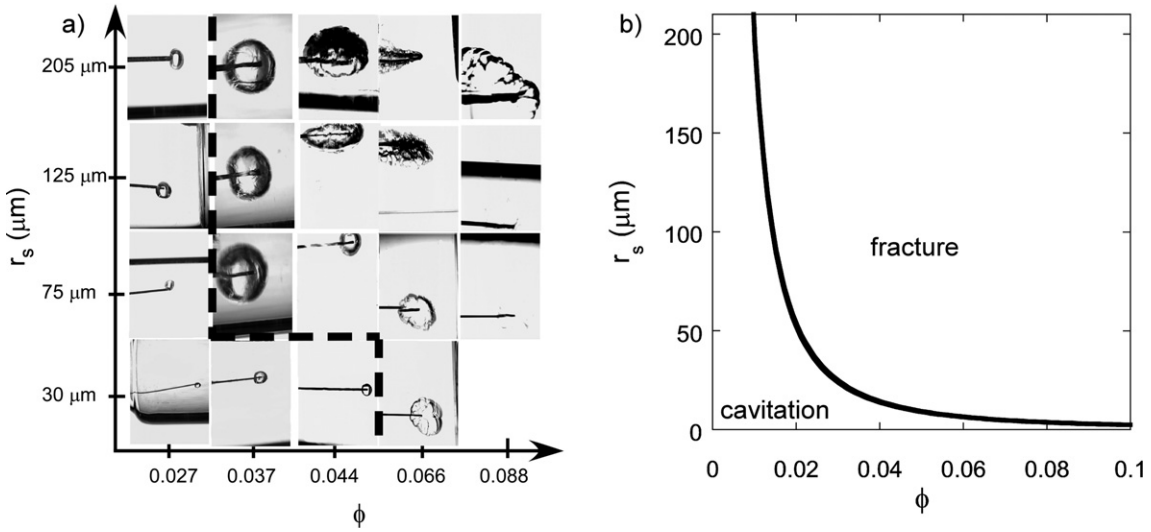

Fig. 7 (a) Micrographs at maximum pressure or the initiation of instability for the gels with different volume fractions. The dotted line indicates the transition from cavitation to fracture. (b) The solid line indicates the model prediction capturing the deformation boundary or transition from cavitation to fracture as a function of volume fraction and syringe radius. Here, $b = 4.5$ Å, $\gamma = 0.072$ J m^{-2}, and $U = 350$ kcal mol^{-1}.

volume fraction, we can understand the measured scaling by recalling that the degree of polymerization between crosslinks, N, will depend upon the polymer volume fraction at crosslinking. As shown in Fig. 5, the best fitting through the data points from the contact mechanics experiments indicates $E \sim \phi^{2.3}$. Therefore, from classical gel mechanics $E \approx (3kT/b^3N)\phi$, and accordingly, $N \sim \phi^{-4/3}$ for the polyacrylamide hydrogels used in these experiments. With this ϕ dependence for N and substituting in the relationship for G_c for good solvent, we obtain:

$$G_c \approx \frac{U}{b^2}\phi^{\frac{5}{24}} \tag{9}$$

which is consistent with our measured data in Fig. 6.

This contrast in volume fraction scaling for E and G_c provides insight into the observed transition from cavitation, *i.e.* elastic, to fracture dominated deformation processes as a function of volume fraction in Fig. 1. The transition from cavitation to fracture can be captured using scaling relationships discussed above to determine the ratio of P_c (eqn (6)) and P_f (eqn (7)) the pressure to cavitate and pressure to fracture, respectively. Substituting $E \approx (3kT/b^3)\phi^{2.3}$ and $G_c \approx (U/b^2)\phi^{5/24}$, the ratio of P_c and P_f, can be shown as:

$$\frac{P_c}{P_f} \approx \frac{5\sqrt{3}}{6}\left(\frac{kT}{U}\right)^{1/2}\left(\frac{r_s}{b}\right)^{1/2}\phi^{25/24} + \frac{2}{\sqrt{3}}\left(\frac{\gamma b^2}{kT}\right)\left(\frac{kT}{U}\right)^{1/2}\left(\frac{b}{r_s}\right)^{1/2}\phi^{-5/4} \tag{10}$$

For $P_c/P_f < 1$, reversible cavitation would be predicted, whereas for $P_c/P_f > 1$ fracture would be predicted. Therefore, we can use the transition condition when $P_c/P_f = 1$ to define a deformation "map" as a function of syringe radius and polymer volume fraction, ϕ, which is plotted in Fig. 7(b). We have considered bond dissociation energy of 350 kcal mol^{-1}, surface energy (γ) of 0.072 J m^{-2}, and the Kuhn length (b) of 4.5 Å. In addition, in Fig. 7(a), we present the micrograph at maximum pressure (or the initiation of instability) for different volume fractions and needle radii. It is evident that cavitation occurs at lower volume fraction and smaller needle radii, consistent with the predicted deformation "map".

Conclusions

In this paper we have adapted scaling theories to capture the reversible and irreversible deformation behavior of a swollen elastic network. The elastic modulus is found to scale strongly with polymer volume fraction, whereas critical energy release rate is a weak function of polymer volume fraction. A simple experimental method involving the pressurization of a syringe needle inserted in a swollen network was used to confirm both predicted trends. The transition from reversible cavitation to irreversible fracture depends on the polymer volume fraction and an initial defect length scale. We anticipate that the cavitation and fracture mechanism investigated here will be widely applicable to soft materials and will significantly enhance the ability to use cavitation measurements to characterize both synthetic and biological materials. In these measurements, the associated length scale is the radius of the syringe needle; therefore, this technique can be used to investigate the local mechanical properties at any arbitrary location across a broad range of length scales from μm to mm.

Acknowledgements

We acknowledge the Center for University of Massachusetts/ Industry Research on Polymers for funding and Dr Guillaume Miquelard-Garnier and Jessica Zimberlin for helpful discussions.

References

1 J. M. S. Renkema and T. van Vliet, *Food Hydrocolloids*, 2004, **18**, 483–487.
2 R. Langer and J. P. Vacanti, *Science*, 1993, **260**, 920–926.
3 Y. Tanaka, R. Kuwabara, Y. H. Na, T. Kurokawa, J. P. Gong and Y. Osada, *J. Phys. Chem. B*, 2005, **109**, 11559–11562.

4 J. A. Stammen, S. Williams, D. N. Ku and R. E. Guldberg, *Biomaterials*, 2001, **22**, 799–806.
5 C. E. Brennen, *Cavitation and Bubble Dynamics*, Oxford University Press, USA, 1995.
6 H. M. James and E. Guth, *J. Polym. Sci.*, 1949, **4**, 153–182.
7 S. P. Obukhov, M. Rubinstein and R. H. Colby, *Macromolecules*, 1994, **27**, 3191–3198.
8 S. V. Panyukov, *Zh. Eksp. Teor. Fiz.*, 1990, **98**, 668–680.
9 P. G. De Gennes, *Scaling Concepts in Polymer Physics*, Cornell Univ. Press, Ithaca, 1979.
10 T. Baumberger, C. Caroli and D. Martina, *Eur. Phys. J. E*, 2006, **21**, 81–89; T. Baumberger, C. Caroli and D. Martina, *Nat. Mater.*, 2006, **5**, 552–555.
11 Y. Tanaka, K. Fukao and Y. Miyamoto, *Eur. Phys. J. E*, 2000, **3**, 395–401.
12 G. J. Lake and A. G. Thomas, *Proc. R. Soc. London, Ser. A*, 1967, **300**, 108–119.
13 J. A. Zimberlin, N. Sanabria-DeLong, G. N. Tew and A. J. Crosby, *Soft Matter*, 2007, **3**, 763–767.
14 A. N. Gent, *Int. J. Non-Linear Mech.*, 2005, **40**, 165–175.
15 Y. Y. Lin and C. Y. Hui, *Int. J. Fracture*, 2004, **126**, 205.
16 A. J. Crosby, M. Hageman and A. Duncan, *Langmuir*, 2005, **21**, 11738–11743; K. L. Johnson, *Contact Mechanics*, Cambridge University Press, Cambridge, UK, 1987; K. R. Shull, *Mater. Sci. Eng. R*, 2002, **36**, 1–45.

